Hind foot drumming: Muscle architecture of the hind limb in three Bathyergidae species

L. Sahd[1], N.C. Bennett[2], S.H. Kotzé[1]

[1] Division of Clinical Anatomy, Department of Biomedical Sciences, Faculty of Medicine and Health Sciences, Stellenbosch University, Cape Town 8000, South Africa

[2] Mammal Research Institute, Department of Zoology and Entomology, University of Pretoria, Pretoria 0002, South Africa

Running Title: Hind limb muscle architecture of Bathyergidae

Editorial correspondence:

Prof S.H. Kotzé

Postal address: Department of Biomedical Sciences, Faculty of Medicine and Health Sciences, Stellenbosch University, PO Box 241, Cape Town, South Africa

Email: shk@sun.ac.za

ABSTRACT

The relationship between muscle architectural properties and hind foot drumming of African mole-rats has yet to be determined using established methodology. Therefore, the internal structure of 32 hind limb muscles was evaluated in two drumming and one non-drumming species of Bathyergidae. The muscle mass (M_M), fascicle length (L_f) and angle of pennation were measured to calculate the physiological cross-sectional area (PCSA) as well as estimate the maximum isometric force of contraction (F_{max}). The most significant differences for the various muscle architecture parameters analyzed in synergistic muscle groups and individual muscles were observed between the rapid drumming *Georychus capensis* and the non-drumming *Cryptomys hottentotus natalensis*. The PCSA values of the hip extensors, hip adductors, knee extensors and knee flexors of *G. capensis* were significantly larger than that of *C. h. natalensis.* Additionally, the hip extensors and knee flexors of both the drumming species (*G. capensis* and *Bathyergus suillus*) were shown to be capable of higher power output compared to the non-drumming species, and the hip adductors of *G. capensis* capable of faster contraction. M. gracilis anticus may play a key role in facilitating hind foot drumming as it was the only muscle to be significantly different in *G. capensis* and *C. h. natalensis* for all three muscle architecture parameters analyzed. Furthermore, it features in the high shortening capacity quadrant of the functional space plot of both *G. capensis* and *B. suillus* but not the non-drumming *C. h. natalensis*.

Keywords:

1.   INTRODUCTION

Seismic signalling is a form of vibrational communication used by a variety of different vertebrate and invertebrate species (Hill 2009; Randall 2010). Seismic signals are transmitted through both the air and ground allowing them to travel long distances (Randall 2001). Foot drumming is one of the most common forms of seismic signalling. Foot drums are produced when the animal strikes the ground with either a single or alternating leg (Randall 2001). Bipedal hind foot drummers such as the kangaroo-rat

(*Dipodomys spectabilis*) balance on their tail while drumming their hind feet by flexion and extension of the ankle joint (Randall 2014). In contrast, quadrupedal hind foot drummers such as African mole-rats, stabilize themselves on their forelimbs while drumming their feet. The drumming is elicited by moving the entire hind limb up and down by flexion and extension of the hip and knee joints (Randall 2014).

Several species of the Bathyergidae family of African mole-rats make use of hind foot drumming whereby they convey territorial and courtship signals (Bennett and Faulkes 2000; Mason and Narins 2001). Narins et al. (1992) and Fransencoli (2000) suggested that the distance between individuals when communicating may influence the use of drumming. These authors surmized that social species living in close quarters were more likely to communicate vocally while solitary species tend to use hind foot drumming for long distance communication. However, Mason and Narins (2010) speculated that the presence or absence of drumming behavior might not be affected by the sociality or differences in environments of a species but rather an inherited behavior from a common ancestor still present in the distinct genera.

Two drumming species of Bathyergidae were examined for this study. Firstly, *Georychus capensis* (Cape mole-rat) is a solitary, chisel tooth digging species found predominantly in the compact hard clay soils of the Western Cape of South Africa (Bennett et al. 2006). Females of this species drum at a rate of 15 beats per second, while males drum at a faster rate of 26 beats per second during courtship (Bennett and Jarvis 1998; Narins et al. 1992; Van Sandwyk and Bennett 2005). Secondly, *Bathyergus suillus* (Cape dune mole-rat) is also a solitary species, a scratch digger, and the largest member of the Bathyergidae family. They display sexual dimorphism with males reaching up to 2 kg in body mass, often double the body mass of females. They are found in sandy soils along coastal areas of the Western Cape, South Africa (Bennett et al. 2009). No exact rate of drumming has been recorded in *B. suillus,* but it has been observed that males can drum rapidly during courtship (Hart et al. 2006). *Cryptomys*

hottentotus natalensis (Natal mole-rat) is a social, chisel tooth digging species found in the compact hard clay soils of the Kwa-Zulu Natal province of South Africa (Hart et al. 2004). Hind foot drumming has not been reported in this sub-species; however, occasional foot stamping has been recorded in other *Cryptomys hottentotus* subspecies (Lacey et al. 2000). It is uncertain if these foot stamps are regarded as seismic signals (Mason and Narins 2010).

Muscle architecture is the principal basis of muscle function (Lieber and Friden 2000). Architectural differences between muscles provide information on muscular force generation as well as the velocity of contraction (Sacks and Roy 1982; Lieber and Friden 2000). Muscle fiber length is considered the most important aspect of muscle architecture (Liber and Ward 2011) as it can influence muscle force predictions. Long muscle fibers have been associated with high contraction velocities (Lieber and Friden 2000; Kikuchi 2010), while fiber length is influenced by the pennation angle of muscles. Pennation angle can vary from parallel to the tendon of insertion to up to a 30° angle with the tendon (Lieber and Friden 2000; Lieber and Ward 2011). The physiological cross-sectional area (PCSA) is calculated using muscle mass, muscle fiber length, and the angle of pennation (Moore et al. 2013) and is the only muscle architectural property that is directly proportional to the isometric force which a muscle is able to generate (Lieber and Ward 2011). Therefore, it is possible that adaptations for hind foot drumming may be reflected in the comparative muscle architecture of the hind limbs in drumming African mole-rat species. Hind limb muscle architecture of rodents is rarely reported and comparisons between a variety of species are scarce. Despite this, the muscle architecture of 29 hind limb muscles in the rat has been reported by Eng et al. (2008) and muscles of the mouse hind limb by Burkholder et al. (1994) and Charles et al.(2016).

The relationship between muscle architectural properties and hind foot drumming of African mole-rats has yet to be determined using established methodology. Therefore, the aim of the present study was to compare the hind limb muscle architecture of two drumming species to a non-drumming species to

determine adaptations for hind foot drumming. It was hypothesized that the muscle architecture of the muscles involved with hind foot drumming such as the hip extensor, knee flexor, and knee extensor muscle groups of the two drumming species would be significantly different to that of the non-drumming *C. h. natalensis*. Musculus gracilis anticus was the only muscle showing a gross anatomical difference between the species studied here (Sahd et al. 2019). Therefore, it was further hypothesized that this muscle would show the most significant differences between the drumming and non-drumming species.

2.   MATERIALS AND METHODS

2.1.   Sample

Hind limbs fixed in 10% buffered formalin of 24 animals consisting of three species (n=8 each, four males and four females per species) were obtained from previous ethically cleared unrelated studies (Table 1). The species included are *G. capensis* (the Cape mole-rat; body mass range: 165 - 337 g), *B. suillus* (the Cape-dune mole-rat; body mass range: 786 - 1290 g), and *C. h. natalensis* (the Natal mole-rat; body mass range: 90 - 191 g). Ethical approval to use the specimens was obtained from the Stellenbosch University Research Ethics Committee: Animal Care and Use (SU-ACUM 16-00005). The limbs were dissected, and the origin and insertion sites of the muscles were determined (Sahd et al. 2019). Thereafter 32 individual muscles were removed from the right hind limb of each sample. In case of damage to the right limb muscles or if joint angulation was not optimal (not 90°), muscles of the left limb were used.

Table 1   Species information including ethical approval, capture information, and mean body mass. (± Standard deviation)

Species	Ethical approval	n	Capture site	Mean body mass (g)
Georychus capensis	University of Johannesburg: 215086650–10/09/15	8	Darling, Western Cape	213.89 ± 60.82
Bathyergus suillus	University of Cape Town: 200/V7/JOR	8	ACSA Cape Town, Western Cape	951.50 ± 191.31
Cryptomys hottentotus natalensis	University of Pretoria: ECO0070–14	8	Glengarry, Kwa-Zulu Natal	118.96 ± 30.63

2.2.   Muscle architecture

Twenty-four limbs in total (n=8 per species) were used for the analysis of muscle architecture. Four architectural parameters were measured in 32 muscles per animal using techniques similar to that described by Payne et al. (2005) in horses and Martin et al. (2019) in a marsupial. Muscle mass (M_M) accurate to the nearest 0.001 g was measured using a digital scale (Ohaus Adventurer Pro AV3102, Nanikon, Switzerland). A digital sliding calliper was used to determine the muscle belly length (L_M) to nearest 0.01 mm. High magnification photographs were taken of each muscle using a Leica MZ67 Stereomicroscope (Leica Biosystems, Wetzlar, Germany). Composite images were generated using Autostich demo version 2.3 (Brown and Louw 2007) after which Image J (Schneider et al. 2012) was used to determine the pennation angle (θ) and fascicle length (L_f) of five randomly chosen fascicles per muscle. The muscle mass and fascicle length of the muscles were corrected using correction factors for fixed muscle tissue (an increase of 14% and 11%, respectively; Kikuch and Kuraoka 2014). Muscle density was determined as 0.001056 g/mm^3 according to Mendez and Keys (1960) and Charles et al. (2016).

The physiological cross-sectional area (PCSA) per muscle was calculated using the formula as described in Sacks and Roy 1982; Charles et al. (2016). Additionally, maximum isometric force of contraction F_{max} of each muscle was estimated by multiplying the PCSA (mm^2) by a maximum isometric stress of 0.3 N/mm^{-2} (Medler 2002). As force is transmitted through the muscle fibers to the muscular matrix and tendon in different ways in different muscles, it is unlikely that this value (0.3 N/mm^{-2}) is consistent across all muscles (Maganaris et al. 1985; Fukunaga et al. 1996). Therefore, the calculation of F_{max} is only an estimation.

$$PCSA\ (mm^2) = \frac{M_M\ (g) \times Pennational\ angle\ (\cos\theta)}{Muscle\ density\ (g/mm^3) \times L_f(mm)}.$$

The ratio of L_f to L_M (L_f/L_M) was used as an architectural index (AI) for comparisons of the individual muscle's capacity for range of contraction and fascicle shortening capability across species and body size (Wickiwicz et al. 1983; Smith et al. 2006; Rupert et al. 2015; Charles et al. 2016). For the purpose of comparison between species, muscles were divided into functional groups based on the classification of muscles in Sahd et al. (2019). Those muscles which have an action on two joints will appear in two muscle groups (Table 2). The hip rotators were studied as individual muscles as in *C. h. natalensis* the m. gluteus profundus could not be removed intact due to the small size. Additionally, m. gracilis posticus was only studied in *C. h. natalensis* as it was not present in the two drumming species (Sahd et al. 2019).

2.3. Statistical Analysis

Descriptive statistics for all measurements and calculations were reported including the mean and standard deviation per species. Ordinary Least Squares (OLS) regressions of log_{10}-transformed data of the M_M, L_f and PCSA for each individual muscle as well as the functional muscle groups were plotted against log_{10} of body mass (M_b) to determine the scaling coefficients for the three species. It was determined that the three species examined here scaled allometrically to body mass for these parameters. Therefore, mixed model analysis of covariance (ANCOVAs) was used to determine significant differences between species as well as sex within a species for both muscle groups and individual muscles. Log_{10}-transformed data were compared with log_{10} body mass (M_b) as the covariate (Myatt et al. 2011). Fischer's Least Significant Difference (LSD) post-hoc test was used to determine the p-values. Statistically significant results were determined with a $p < 0.05$. All statistical analysis was performed using Statistica 13.5 (TIBCO software, Palo Alto, California, USA). All graphs were created in ggplot2 (Wickham 2016) in R (R core team 2013).

Table 2 The muscle function groups used for analysis

Muscle Group	Muscle
Hip flexors (HF)	M. iliacus
	M. psoas major
	M. pectineus
	M. rectus femoris
Hip extensors (HE)	M. gluteus superficialis
	M. gluteus medius
	M. semitendinosus
	M. biceps femoris
	M. semimembranosus
	M. gluteofemoralis
Hip rotators (Studied as individual muscles as in *C. h. natalensis* the m. gluteus profundus could not be removed intact due to the small size)	M. gluteus profundus
	M. piriformis
Hip adductors (HA)	M. adductor brevis
	M. gracilis anticus
	M. gracilis posticus
	(only in *C .h. natalensis*)
	M. adductor longus
	M. adductor magnus
Knee extensors (KE)	M. vastus lateralis
	M. vastus medialis
	M. vastus intermedius
	M. rectus femoris
Knee flexors (KF)	M. semitendinosus
	M. biceps femoris
	M. semimembranosus
	M. gracilis anticus
	M. adductor longus
	M. gastrocnemius
	M. plantaris
Ankle dorsiflexors (ADF)	M. tibialis cranialis
	M. extensor digitorum longus
	M. extensor hallucis longus
Ankle plantar flexors (APF)	M. gastrocnemius
	M. soleus
	M. plantaris
	M. flexor hallucis longus
	M. tibialis caudalis
Ankle evertors (AE)	M. peroneus longus
	M. peroneus brevis

2.4 Functional space plots

The scatter plots of the mean PCSA (normalized to body mass, $PCSA/M_b^{0.67}$) of each muscle group as well as individual muscles were plotted against the mean L_f (normalized to body mass, $L_f/M_b^{0.33}$) in each species. These figures show the functional space plots of the muscle groups thereby giving an estimation of the relative muscle function (Allen et al. 2010). As there was a large size variation between

species, the normalization of parameters to body mass assumed geometric isometry to allow for ease of comparison between species. The data that support the findings of this study are available from the corresponding author upon reasonable request.

3.   RESULTS

The means and standard deviations for each muscle architecture parameter of each individual muscle are detailed per species in Tables 3-8. The mean belly length, muscle mass, and Fmax of each muscle group per species are indicated in Figure 1(A-C). Of the 32 muscles studied, nine muscles were unipennate in *C. h. natalensis*, and eight in both *G. capensis* and *B. suillus*, respectively. The angle of pennation of all the pennate muscles examined (except for m. gluteus superficialis in all three species and m. piriformis in *G. capensis*) was less than 20°.

Table 3   The mean and standard deviation of the muscle architecture parameters of the proximal hind limb muscles of *Georychus capensis*

Muscle	Abbr.	n	Muscle mass (M_m, g)	Belly length (L_M, mm)	Fascicle length (L_f, mm)	Physiological cross-sectional area (PCSA, mm^2)	Angle of pennation $(\theta, °)$	F_{max} (N/mm^{-2})
Iliacus	I	7	0.27 ± 0.08	19.27 ± 3.44	14.51 ± 2.40	16.94 ± 3.33	6.84 ± 5.49	5.08 ± 1.00
Psoas major	PM	7	0.24 ± 0.10	21.29 ± 3.85	13.29 ± 4.22	18.83 ± 10.23	13.38 ± 3.77	5.65 ± 3.07
Pectineus	P	8	0.07 ± 0.04	14.70 ± 2.11	10.16 ± 1.66	6.63 ± 3.06	7.53 ± 7.82	1.99 ± 0.92
Vastus lateralis	VL	8	0.36 ± 0.13	28.58 ± 4.27	17.44 ± 2.76	19.88 ± 8.84	16.19 ± 4.42	5.96 ± 2.65
Vastus medialis	VM	8	0.24 ± 0.10	23.99 ± 2.70	15.07 ± 1.70	14.54 ± 5.57	13.60 ± 3.47	4.36 ± 1.67
Vastus intermedius	VI	8	0.21 ± 0.112	26.14 ± 1.21	17.46 ± 1.34	11.00 ± 5.62	12.18 ± 4.39	3.30 ± 1.69
Rectus femoris	RF	8	0.81 ± 0.35	28.18 ± 2.33	18.86 ± 2.13	37.99 ± 13.70	18.19 ± 7.08	12.54 ± 4.52
Gluteus superficialis	GS	8	0.58 ± 0.27*	20.16 ± 4.29	18.30 ± 3.63	16.29 ± 3.95	54.88 ± 6.32	4.89 ± 1.19
Gluteus medius	GMED	8	0.35 ± 0.18	18.82 ± 2.20	11.94 ± 1.72§	26.96 ± 14.90	15.95 ± 3.73	8.09 ± 4.47
Gluteus profundus	GMIN	7	0.09 ± 0.05	14.81 ± 2.16	8.35 ± 1.03	9.92 ± 4.84	16.56 ± 2.20	2.98 ± 1.45
Piriformis	PI	8	0.30 ± 0.13	19.90 ± 1.26	9.73 ± 1.01	26.85 ± 2.06*	23.40 ± 7.77	8.05 ± 3.35
Semitendinosus	ST	8	0.49 ± 0.25*	26.52 ± 3.73	26.14 ± 3.60	17.47 ± 7.50*	0.00 ± 0.00	5.24 ± 2.25
Biceps femoris cranial head	BFAN	8	0.51 ± 0.16*§	33.40 ± 3.80	29.54 ± 3.21	16.53 ± 5.55	0.00 ± 0.00	4.96 ± 1.67
Biceps femoris caudal head	BFAC	8	0.36 ± 0.21	25.07 ± 5.03	21.55 ± 4.07	15.15 ± 5.65	0.00 ± 0.00	4.54 ± 1.70
Semimembranosus	SM	8	0.68 ± 0.18*§	32.09 ± 5.30	29.41 ± 5.27	22.79 ± 8.85	0.00 ± 0.00	6.84 ± 2.66
Gluteofemoralis	GF	8	0.35 ± 0.11*	28.41 ± 4.25	25.57 ± 4.26	13.34 ± 4.62*	0.00 ± 0.00	4.00 ± 1.39
Adductor brevis	AB	8	0.39 ± 0.16	30.80 ± 5.55	28.58 ± 4.44	12.65 ± 3.52	0.00 ± 0.00	3.79 ± 1.06
Gracilis anticus	GA	8	0.54 ± 0.22*	25.48 ± 4.05	24.43 ± 3.90*	20.89 ± 6.50*	0.00 ± 0.00	6.27 ± 1.95
Adductor longus	AL	8	0.12 ± 0.07	18.79 ± 3.44	13.82 ± 3.07	8.00 ± 3.72	0.50 ± 1.40	2.40 ± 1.12
Adductor magnus	AM	8	0.29 ± 0.12	23.50 ± 3.08	19.08 ± 3.11	14.74 ± 6.46	1.74 ± 3.32	4.42 ± 1.94

* indicates statistically significant difference to *C. h. natalensis*, § indicates statistically significant difference to *B. suillus*

Table 4 The mean and standard deviation of the muscle architecture parameters of the distal hind limb muscles of *Georychus capensis*

Muscle	Abbr.	n	Muscle mass (M_m, g)	Belly length (L_M, mm)	Fascicle length (L_f, mm)	Physiological cross-sectional area (PCSA, mm^2)	Angle of pennation (θ, °)	F_{max} (N/mm^{-2})
Tibialis cranialis	TA	8	0.16 ± 0.05	16.36 ± 1.78	13.41 ± 1.56*§	11.35 ± 4.51	16.20 ± 3.11	3.40 ± 1.35
Extensor digitorium longus	EDL	8	0.06 ± 0.03	17.72 ± 1.90	14.53 ± 2.91	4.08 ± 2.26	10.37 ± 4.54	1.22 ± 0.68
Extensor hallucis longus	EHL	8	0.05 ± 0.02	13.50 ± 1.39	10.79 ± 1.62	4.52 ± 1.47	16.67 ± 7.32	1.36 ± 0.44
Gastrocnemius medial head	GCM	8	0.21 ± 0.08*	15.40 ± 1.35	12.58 ± 2.46	16.42 ± 8.79	12.02 ± 2.15	4.93 ± 2.64
Gastrocnemius lateral head	GCL	8	0.23 ± 0.06*	16.88 ± 1.85	13.09 ± 1.41	15.81 ± 3.81*	17.17 ± 7.16	4.74 ± 1.14
Soleus	S	8	0.03 ± 0.02§	11.92 ± 2.59	10.41 ± 3.08	2.72 ± 2.38	19.75 ± 7.35	0.82 ± 0.71
Plantaris	PLA	8	0.11 ± 0.04	15.45 ± 1.91	12.51 ± 1.41	7.88 ± 3.34	16.72 ± 4.82	2.36 ± 1.00
Flexor hallucis longus	FHL	8	0.04 ± 0.01	13.43 ± 1.06	8.43 ± 3.65	5.11 ± 3.21	16.17 ± 3.31	1.53 ± 0.96
Tibialis caudalis	TP	8	0.07 ± 0.03	14.29 ± 1.84	10.26 ± 2.85	7.39 ± 4.38	12.68 ± 4.02	2.22 ± 1.31
Peroneus longus	PL	8	0.04 ± 0.01	13.47 ± 1.57	10.08 ± 3.23	4.06 ± 1.70	12.88 ± 3.15	1.22 ± 0.51
Peroneus brevis	PB	7	0.05 ± 0.02	12.66 ± 1.38	8.36 ± 2.12	5.83 ± 2.73	13.16 ± 3.76	1.75 ± 0.82

* indicates statistically significant difference to *C. h. natalensis*, § indicates statistically significant difference to *B. suillus*

Table 5 The mean and standard deviation of the muscle architecture parameters of the proximal hind limb muscles of *Bathyergus suillus*

Muscle	Abbr.	n	Muscle mass (M_m, g)	Belly length (L_M, mm)	Fascicle length (L_f, mm)	Physiological cross-sectional area (PCSA, mm^2)	Angle of pennation (θ, °)	F_{max} (N/mm^{-2})
Iliacus	I	7	1.44 ± 0.53	33.15 ± 4.77	21.94 ± 4.73	59.84 ± 17.59	10.77 ± 5.51	17.95 ± 5.28
Psoas major	PM	7	1.26 ± 0.55	41.86 ± 9.96	20.95 ± 5.33	57.31 ± 27.26	13.09 ± 9.23	17.19 ± 8.18
Pectineus	P	8	0.36 ± 0.15	21.81 ± 2.07	14.61 ± 2.70*¥	24.12 ± 13.07	7.09 ± 5.52	7.24 ± 3.92
Vastus lateralis	VL	8	1.95 ± 0.54	47.90 ± 4.73	30.09 ± 4.91	60.97 ± 20.37	15.79 ± 4.65	18.29 ± 6.11
Vastus medialis	VM	8	1.20 ± 0.43	42.34 ± 3.64	24.25 ± 6.15	47.62 ± 20.65	12.94 ± 5.45	14.29 ± 6.19
Vastus intermedius	VI	8	0.97 ± 0.36	38.77 ± 8.55	26.82 ± 6.23	32.92 ± 10.88	17.90 ± 7.53	9.88 ± 3.26
Rectus femoris	RF	8	5.06 ± 1.22	45.60 ± 3.92	31.32 ± 4.69	147.91 ± 42.55	18.20 ± 5.12	48.81 ± 14.04
Gluteus superficialis	GS	8	3.73 ± 0.99	35.36 ± 6.44	32.82 ± 4.18	49.01 ± 35.07	61.61 ± 18.78	14.70 ± 10.52
Gluteus medius	GMED	8	1.64 ± 0.47	33.22 ± 4.04	24.39 ± 6.96*¥	65.20 ± 26.55	15.81 ± 4.72	19.56 ± 7.96
Gluteus profundus	GMIN	8	0.53 ± 0.26	27.87 ± 2.50	15.09 ± 2.33	32.28 ± 16.88	14.71 ± 5.16	9.68 ± 5.07
Piriformis	PI	8	1.15 ± 0.40	32.54 ± 5.91	21.04 ± 5.52	49.20 ± 16.35	17.91 ± 5.42	14.76 ± 4.90
Semitendinosus	ST	8	2.20 ± 0.67	52.32 ± 8.80	49.13 ± 9.99	42.44 ± 10.05	0.00 ± 0.00	12.73 ± 3.02
Biceps femoris cranial head	BFAN	8	3.35 ± 0.82*¥	56.61 ± 2.88	52.76 ± 6.92	60.47 ± 15.28	0.00 ± 0.00	18.14 ± 4.58
Biceps femoris caudal head	BFAC	8	1.62 ± 0.35	36.37 ± 4.13	30.76 ± 4.37	50.98 ± 13.77	0.00 ± 0.00	15.30 ± 4.13
Semimembranosus	SM	8	4.29 ± 0.93*¥	53.89 ± 4.92	54.20 ± 5.82	74.46 ± 11.41	0.00 ± 0.00	22.34 ± 3.42
Gluteofemoralis	GF	8	1.66 ± 0.65	48.05 ± 3.28	46.58 ± 5.21	33.65 ± 12.32	0.00 ± 0.00	10.09 ± 3.70
Adductor brevis	AB	7	2.71 ± 0.78	47.52 ± 5.83	42.61 ± 8.29	62.43 ± 21.79	0.00 ± 0.00	18.73 ± 6.54
Gracilis anticus	GA	8	3.19 ± 0.81*	38.15 ± 4.06	36.03 ± 4.72	84.50 ± 22.26	0.00 ± 0.00	25.35 ± 6.68
Adductor longus	AL	8	0.38 ± 0.20	26.83 ± 3.50	20.89 ± 2.72	16.93 ± 7.36	0.71 ± 2.02	5.08 ± 2.21
Adductor magnus	AM	8	1.82 ± 0.51	36.16 ± 4.79	28.24 ± 5.66	61.64 ± 16.37	1.17 ± 7.45	18.49 ± 4.91

* indicates a statistically significant difference to *C. h. natalensis*, ¥ indicates a statistically significant difference to *G. capensis*

Table 6 The mean and standard deviation of the muscle architecture parameters of the distal hind limb muscles of *Bathyergus suillus*

Muscle	Abbr.	n	Muscle mass (M_m, g)	Belly length (L_M, mm)	Fascicle length (L_f, mm)	Physiological cross-sectional area (PCSA, mm^2)	Angle of pennation (θ, °)	F_{max} (N/mm^{-2})
Tibialis cranialis	TA	8	0.87 ± 0.21	27.82 ± 2.72	24.63 ± 3.45*¥	31.59 ± 6.90	17.42 ± 5.46	9.48 ± 2.07
Extensor digitorium longus	EDL	8	0.39 ± 0.07	34.12 ± 3.31	26.19 ± 4.62	13.09 ± 2.36	13.06 ± 5.65	4.11 ± 0.71
Extensor hallucis longus	EHL	8	0.27 ± 0.07	24.44 ± 2.27	19.91 ± 4.28	12.50 ± 4.08	15.73 ± 7.54	3.75 ± 1.22
Gastrocnemius medial head	GCM	7	1.20 ± 0.28*	27.33 ± 4.45	22.59 ± 3.99	48.97 ± 6.84	11.44 ± 3.78	14.69 ± 2.05
Gastrocnemius lateral head	GCL	7	0.93 ± 0.30*	27.07 ± 3.80	22.21 ± 2.23	38.49 ± 12.59	14.41 ± 3.55	11.55 ± 3.78
Soleus	S	8	0.30 ± 0.13¥	22.13 ± 4.41	17.14 ± 4.85	15.77 ± 4.12	13.73 ± 2.57	4.73 ± 1.24
Plantaris	PLA	8	0.54 ± 0.13	27.38 ± 5.19	24.43 ± 5.80	20.50 ± 4.40	15.54 ± 6.03	6.15 ± 1.32
Flexor hallucis longus	FHL	8	0.23 ± 0.12	21.61 ± 3.18	15.23 ± 6.28	15.06 ± 8.392	16.79 ± 7.32	4.52 ± 2.24
Tibialis caudalis	TP	8	0.25 ± 0.06	22.31 ± 3.51	13.54 ± 2.22	16.93 ± 5.29	13.92 ± 4.34	5.08 ± 1.59
Peroneus longus	PL	8	0.28 ± 0.16	22.81 ± 2.82	16.41 ± 2.59	15.90 ± 8.36	10.27 ± 2.18	4.77 ± 2.51
Peroneus brevis	PB	8	0.25 ± 0.12	21.44 ± 3.77	16.45 ± 1.74	13.59 ± 6.62	13.55 ± 4.96	4.08 ± 1.99

* indicates a statistically significant difference to *C. h. natalensis*, ¥ indicates a statistically significant difference to *G. capensis*

Table 7 The mean and standard deviation of the muscle architecture parameters of the proximal hind limb muscles of *Cryptomys hottentotus natalensis*

Muscle	Abbr.	n	Muscle mass (M_m, g)	Belly length (L_M, mm)	Fascicle length (L_f, mm)	Physiological cross-sectional area (PCSA, mm^2)	Angle of pennation (θ, °)	F_{max} (N/mm^{-2})
Iliacus	I	7	0.09 ± 0.02	13.31 ± 2.01	10.81 ± 2.25	8.42 ± 2.74	15.63 ± 8.27	2.53 ± 0.82
Psoas major	PM	7	0.10 ± 0.10	18.60 ± 5.23	11.35 ± 1.15	8.50 ± 8.84	15.10 ± 6.28	2.55 ± 2.65
Pectineus	P	7	0.04 ± 0.03	12.36 ± 3.13	10.79 ± 3.16§¥	4.94 ± 2.81	3.81 ± 3.36	1.48 ± 0.84
Vastus lateralis	VL	8	0.13 ± 0.04	20.65 ± 1.71	16.05 ± 2.47	7.47 ± 2.74	13.40 ± 3.46	2.24 ± 0.82
Vastus medialis	VM	8	0.07 ± 0.04	18.92 ± 3.12	14.49 ± 1.98	4.54 ± 2.09	13.72 ± 5.07	1.36 ± 0.63
Vastus intermedius	VI	8	0.07 ± 0.04	16.34 ± 2.58	13.25 ± 1.92	5.18 ± 2.46	13.21 ± 2.98	1.55 ± 0.74
Rectus femoris	RF	8	0.31 ± 0.11	19.22 ± 1.88	14.15 ± 1.43	20.27 ± 6.78	17.41 ± 4.73	6.69 ± 2.24
Gluteus superficialis	GS	8	0.16 ± 0.06¥	13.76 ± 1.44	14.18 ± 1.99	6.76 ± 1.84	47.27 ± 9.79	2.03 ± 0.55
Gluteus medius	GMED	8	0.11 ± 0.04	14.96 ± 1.48	11.64 ± 1.49§	9.12 ± 3.65	14.51 ± 4.77	2.74 ± 1.10
Piriformis	PI	8	0.09 ± 0.03	14.86 ± 1.70	11.20 ± 2.84	7.97 ± 2.06¥	13.13 ± 5.33	2.39 ± 0.62
Semitendinosus	ST	7	0.15 ± 0.04¥	20.35 ± 1.52	19.75 ± 2.05	7.30 ± 1.97¥	0.00 ± 0.00	2.19 ± 0.59
Biceps femoris cranial head	BFAN	8	0.18 ± 0.04§¥	25.19 ± 1.99	25.01 ± 2.50	6.79 ± 1.04	0.00 ± 0.00	2.04 ± 0.31
Biceps femoris caudal head	BFAC	8	0.19 ± 0.06	18.65 ± 3.00	17.04 ± 1.85	10.25 ± 3.14	0.00 ± 0.00	3.08 ± 0.94
Semimembranosus	SM	8	0.23 ± 0.08§¥	22.97 ± 2.00	23.04 ± 3.62	9.50 ± 3.29¥	0.00 ± 0.00	2.85 ± 0.99
Gluteofemoralis	GF	7	0.10 ± 0.02¥	20.85 ± 2.27	21.22 ± 3.75	4.31 ± 1.23¥	0.00 ± 0.00	1.29 ± 0.37
Adductor brevis	AB	8	0.15 ± 0.06	22.91 ± 2.42	20.89 ± 3.47	6.26 ± 1.97	0.00 ± 0.00	1.88 ± 0.59
Gracilis anticus	GA	8	0.08 ± 0.03§¥	15.82 ± 2.07	14.60 ± 1.22¥	4.94 ± 1.50¥	0.00 ± 0.00	1.48 ± 0.45
Gracilis posticus	GP	8	0.07 ± 0.02	15.36 ± 1.08	15.27 ± 1.01	4.57 ± 0.87	0.00 ± 0.00	1.37 ± 0.26
Adductor longus	AL	6	0.04 ± 0.02	14.43 ± 4.22	14.20 ± 4.46	2.64 ± 1.26	0.00 ± 0.00	0.79 ± 0.38
Adductor magnus	AM	8	0.11 ± 0.04	17.01 ± 1.83	14.44 ± 2.08	7.97 ± 3.16	6.43 ± 4.90	2.39 ± 0.95

§ indicates statistically significant difference to *B. suillus*, ¥ indicates statistically significant difference to *G. capensis*

Table 8 The mean and standard deviation of the muscle architecture parameters of the distal hind limb muscles of *Cryptomys hottentotus natalensis*

Muscle	Abbr.	n	Muscle mass (M_m, g)	Belly length (L_M, mm)	Fascicle length (L_f, mm)	Physiological cross-sectional area (PCSA, mm^2)	Angle of pennation (θ, °)	F_{max} (N/mm^{-2})
Tibialis cranialis	TA	8	0.08 ± 0.02	11.41 ± 1.00	9.93 ± 1.17[§¥]	7.43 ± 1.50	14.38 ± 5.05	2.23 ± 0.45
Extensor digitorium longus	EDL	8	0.04 ± 0.02	13.74 ± 1.36	11.62 ± 2.58	3.06 ± 1.11	10.02 ± 2.67	0.92 ± 0.33
Extensor hallucis longus	EHL	8	0.03 ± 0.02	10.29 ± 1.16	8.69 ± 2.02	3.38 ± 2.00	14.02 ± 4.19	1.01 ± 0.60
Gastrocnemius medial head	GCM	7	0.07 ± 0.02[§¥]	12.08 ± 1.09	10.40 ± 2.11	6.89 ± 1.35	9.46 ± 2.00	2.07 ± 0.40
Gastrocnemius lateral head	GCL	7	0.07 ± 0.02[§¥]	12.08 ± 1.50	11.11 ± 1.76	6.00 ± 1.12[¥]	15.98 ± 9.52	1.80 ± 0.34
Soleus	S	8	0.02 ± 0.01	10.24 ± 1.70	10.71 ± 1.73	1.95 ± 1.01	12.63 ± 4.85	0.59 ± 0.30
Plantaris	PLA	8	0.05 ± 0.01	10.86 ± 1.33	10.98 ± 1.37	4.10 ± 1.14	12.48 ± 4.94	1.23 ± 0.34
Flexor hallucis longus	FHL	8	0.02 ± 0.01	10.17 ± 0.55	7.69 ± 1.70	2.61 ± 1.21	14.69 ± 5.60	0.78 ± 0.36
Tibialis caudalis	TP	7	0.03 ± 0.02	10.57 ± 1.95	7.60 ± 0.81	3.96 ± 2.74	13.03 ± 4.11	1.19 ± 0.82
Peroneus longus	PL	8	0.03 ± 0.01	10.58 ± 2.01	7.66 ± 2.03	3.19 ± 1.44	13.55 ± 3.23	0.96 ± 0.43
Peroneus brevis	PB	8	0.02 ± 0.01	9.31 ± 1.15	8.10 ± 1.24	3.09 ± 1.05	12.24 ± 5.56	0.93 ± 0.32

[§] indicates statistically significant difference to *B. suillus*, [¥] indicates statistically significant difference to *G. capensis*
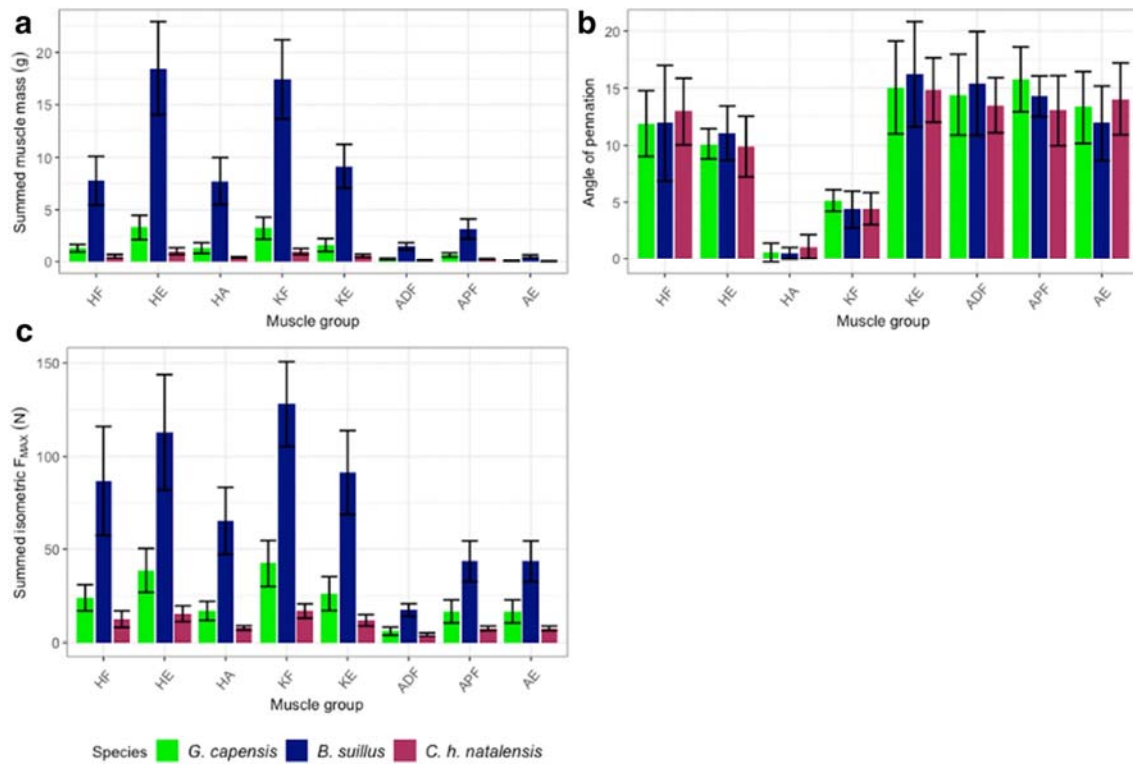

Figure 1. Mean (± standard error) of various muscle architecture parameters namely, muscle mass (**A**), angle of pennation (**B**), and maximum isometric force (**C**) of the muscle groups of *G. capensis*, *B. suillus*, and *C. h. natalensis*. Muscle group abbreviations: Hip flexors (HF), Hip extensors (HE), Hip adductors (HA), Knee extensors (KE), Knee flexors (KF), Ankle dorsiflexors (ADF), Ankle plantar flexors (APF), and Ankle evertors (AE).

The hind limb muscle mass of all three species was distributed in a proximal-distal gradient with the larger muscles originating near the hip joint (except for m. pectineus). The hip extensor muscle group comprised the largest percentage of the total hind limb muscle mass. The knee flexors were the second largest muscle group encompassing up to $39.46 \pm 2.98\%$ of the total hind limb mass. This was followed by the knee extensor, the hip flexor, and the hip adductor muscle groups each comprising of 16 to 20% of the total hind limb muscle mass. The remaining three muscle groups each contributed less than 10% to the total hind limb M_M (Fig. 2).
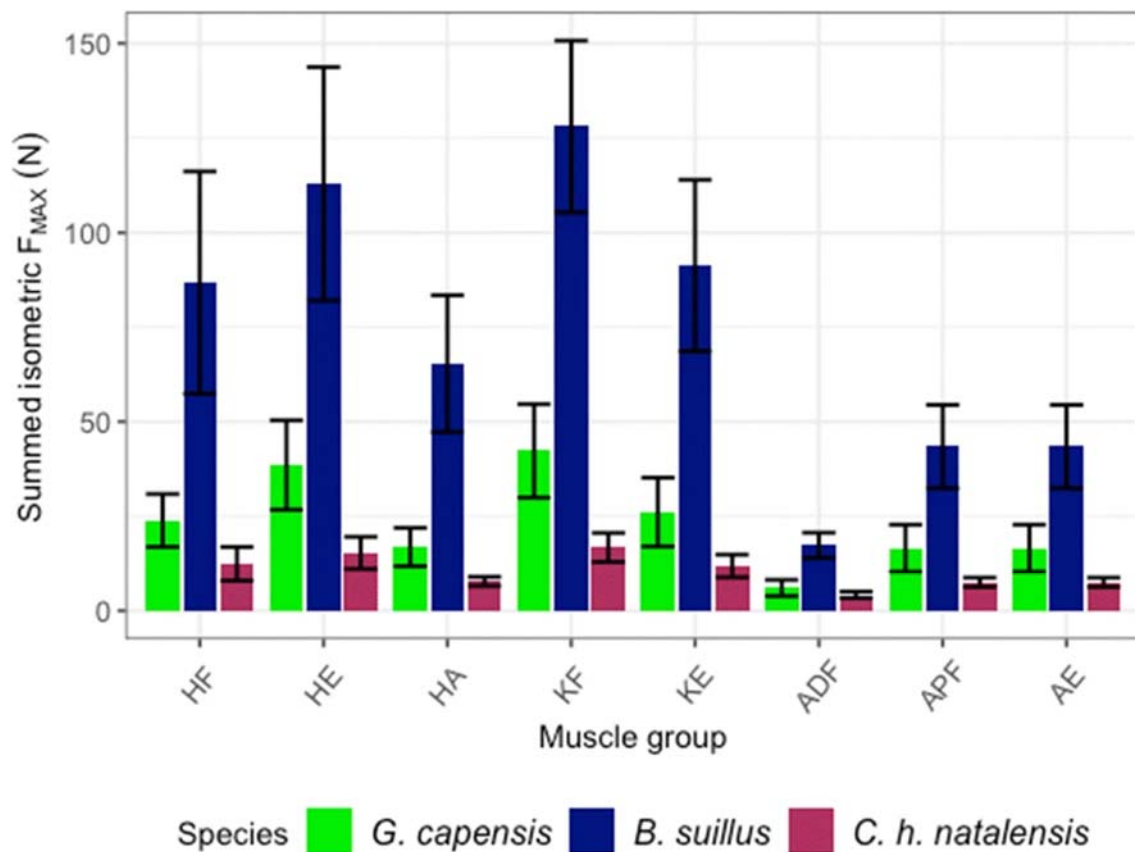
Figure 2. Distribution of the muscle mass of each functional muscle group to the total hind limb muscle mass of *G. capensis*, *B. suillus*, and *C. h. natalensis*. Total hind limb mass was calculated as the summed mass of all individual muscles. Proximal to distal muscle group mass is expressed as a percentage, with the bars representing the mean and the error bars representing the standard deviation for each muscle group. Biarticular muscles are included in more than one group. Muscle group abbreviations: Hip flexors (HF), Hip extensors (HE), Hip adductors (HA), Knee extensors (KE), Knee flexors (KF), Ankle dorsiflexors (ADF), Ankle plantarflexors (APF), and Ankle evertors (AE).

3.1 Muscle architecture comparisons of muscle groups

Results of the ANCOVA analysis, including the p-values, for differences between species are detailed in Table 9. No sex differences within a species were observed in the muscle groups.

Table 9 The analysis of covariance (ANCOVA) results of the comparisons of the muscle groups between species

Muscle group	Muscle mass (M_m)			Fascicle length (l_f)			Physiological cross-sectional area (pcsa)		
	F	df	P	F	df	P	F	df	P
Hip flexors	26.75	2	.63	3.64	2	.06	1.38	2	.28
Hip extensors	**7.235**	2	**p <.01**	2.63	2	.10	**4.31**	2	**.03**
Hip adductors	**6.41**	2	**.01**	1.60	2	.23	**4.72**	2	**.02**
Knee flexors	**6.57**	2	**.01**	3.02	2	.08	**6.27**	2	**.01**
Knee extensors	**4.88**	2	**.02**	1.83	2	.19	**4.22**	2	**.03**
Ankle dorsiflexors	2.64	2	.10	**5.58**	2	**.01**	0.69	2	.51
Ankle plantarflexors	**4.00**	2	**.04**	2.43	2	.12	0.92	2	.69
Ankle evertors	2.15	2	.15	1.90	2	.18	0.21	2	.81

Bold text indicates significant results p < 0.05

3.1.1 Fascicle length (L_f)

Trends were observed in the L_f of the hip flexor, hip extensor and knee flexor muscle groups. *Bathyergus suillus* had the longest fascicles compared to both other species in the hip and knee flexors. Additionally, *B. suillus* had the longest fascicles compared to *G. capensis* of the hip extensors. The ankle dorsiflexors were significantly different in all three species with *B. suillus* having the longest fascicles and *C. h. natalensis* the shortest.

3.1.2. Muscle mass (M_M)

The M_M of the hip extensors and knee flexors in *C. h. natalensis* were significantly smaller compared to both drumming species. Additionally, the hip adductors and knee extensors of *G. capensis* had significantly larger M_M values compared to *C. h. natalensis*. The M_M of the ankle plantar flexors of all three species were significantly different where *B. suillus* had the heaviest plantar flexors and *C. h. natalensis* the lightest.

3.1.3. Physiological cross-sectional area (PCSA)

The PCSA values of the hip extensors, hip adductors, knee extensors, and knee flexors of *G. capensis* were significantly larger than that of *C. h. natalensis*.

3.1.4 Functional space plot

The mean PCSA (normalized to mass, $PCSA/M_b^{0.67}$) of each muscle group is plotted against the mean L_f (normalized to mass, $L_f/M_b^{0.33}$) per species in Figure 3. This figure shows the functional space plots of the muscle groups thereby giving an estimation of the relative muscle function (Allen et al. 2010). The hip extensors and knee flexors of the drumming species are in the upper right quadrant indicating that they are capable of high-power output. However, the hip adductors of *G. capensis* had longer normalized fascicles extending farther into the lower right quadrant indicating that they are possibly adapted for increased shortening capacity and simultaneous greater range of motion.
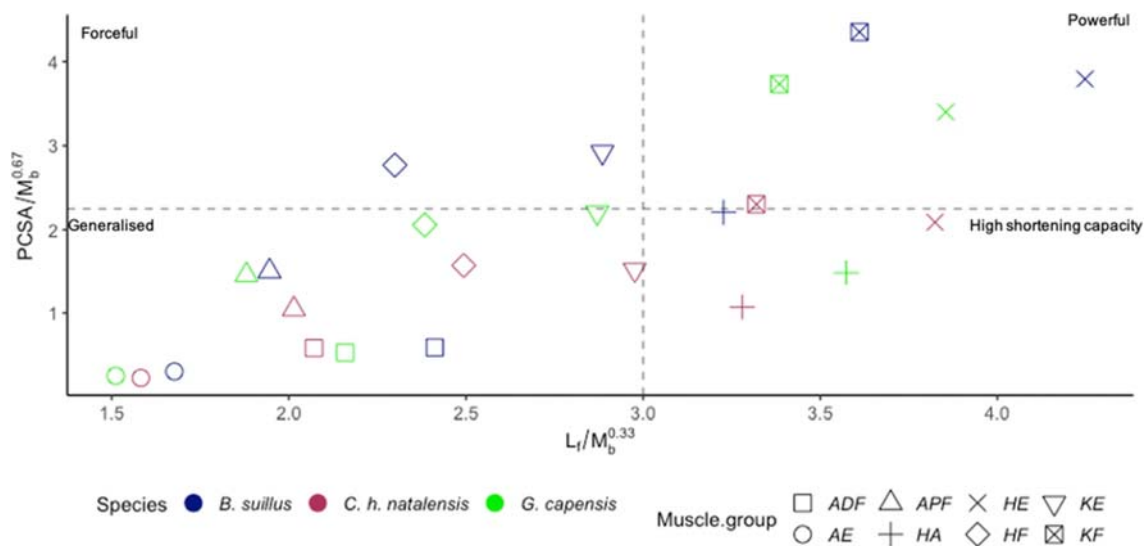
Figure 3. Physiological cross-sectional area, normalized to body mass ($PCSA/BM^{0.67}$) as a function of resting fascicle length normalized to body mass ($LF/BM^{0.33}$) of the muscle groups in *G. capensis*, *B. suillus*, and *C. h. natalensis*. The horizontal dashed line separates muscles with high (above) versus low (below) force capability, while the vertical dashed line separates muscles with high (right) versus low (left) shortening capability. Muscles with both high force and high shortening capabilities are thus adapted for high-power outputs (right upper quadrant). Muscle group abbreviations: Hip flexors (HF), Hip extensors (HE), Hip adductors (HA), Knee extensors (KE), Knee flexors (KF), Ankle dorsiflexors (ADF), Ankle plantar flexors (APF), and Ankle evertors (AE).

3.1. Muscle architecture comparison of individual muscles

Results of the ANCOVA analysis, including the p-values, for differences between species are detailed in Tables 10 and 11 (proximal and distal muscles, respectively). Tables 3-8 indicate the specific species differences.

Table 10 The analysis of covariance (ANCOVA) results of the comparisons of the proximal individual muscles between species

Muscle	Muscle mass (M_m)			Fascicle length (L_f)			Physiological cross-sectional area (PCSA)			L_f/L_m		
	F	df	P	F	df	P	F	df	P	F	df	P
Iliacus	3.79	2	.05	2.32	2	.14	2.17	2	.15	0.15	2	.86
Psoas major	1.65	2	.23	0.11	2	.89	1.39	2	.28	0.18	2	.84
Pectineus	0.60	2	.56	**8.36**	**2**	***p<.01***	0.95	2	.41	2.86	2	.09
Vastus lateralis	2.51	2	.11	1.51	2	.25	1.94	2	.17	3.07	2	.07
Vastus medialis	2.61	2	.10	0.44	2	.65	**3.97**	**2**	**.04**	1.03	2	.38
Vastus intermedius	1.12	2	.35	1.73	2	.21	0.48	2	.63	**6.06**	**2**	**.01**
Rectus femoris	0.47	2	.63	1.66	2	.22	0.02	2	.98	0.98	2	.40
Gluteus superficialis	**6.11**	**2**	**.01**	0.08	2	.93	1.55	2	.24	1.67	2	.22
Gluteus medius	3.60	2	.05	**5.08**	**2**	**.02**	3.69	2	.05	**4.43**	**2**	**.03**
Gluteus profundus	0.18	2	.68	0.05	2	.83	0.16	2	.70	0.07	2	.79
Piriformis	3.17	2	.07	**4.39**	**2**	**.03**	**7.75**	**2**	**p<.01**	**8.96**	**2**	**p<.01**
Semitendinosus	**8.76**	**2**	**p<.01**	0.01	2	.99	**7.08**	**2**	**.01**	1.72	2	.21
Biceps femoris cranial head	**4.71**	**2**	**.02**	2.09	2	.15	3.72	2	.05	1.64	2	.22
Biceps femoris caudal head	0.30	2	.74	0.70	2	.51	0.44	2	.65	0.18	2	.84
Semimembranosus	**6.93**	**2**	**.01**	1.09	2	.36	2.88	2	.08	**4.38**	**2**	**.03**
Gluteofemoralis	**7.42**	**2**	**.01**	1.53	2	.20	**5.48**	**2**	**.02**	**7.46**	**2**	**.01**
Adductor brevis	1.02	2	.38	1.07	2	.37	1.40	2	.28	0.96	2	.40
Gracilis anticus	**41.61**	**2**	**p<.01**	**9.03**	**2**	**p<.01**	**20.07**	**2**	**p<.01**	0.19	2	.83
Adductor longus	1.80	2	.20	1.27	2	.31	**4.21**	**2**	**.04**	**4.05**	**2**	**.04**
Adductor magnus	0.78	2	.47	0.65	2	.53	0.28	2	.76	0.06	2	.94

Bold text indicates significant results $p < 0.05$

Table 11 The analysis of covariance (ANCOVA) results of the comparisons of the distal individual muscles between species

Muscle	Muscle mass (M_m)			Fascicle length (L_f)			Physiological cross-sectional area (PCSA)			L_f/L_m		
	F	df	P	F	df	P	F	df	P	F	df	P
Tibialis cranialis	1.26	2	.31	**6.94**	**2**	**.01**	0.18	2	.84	2.60	2	.10
Extensor digitorium longus	2.21	2	.14	0.48	2	.63	1.20	2	.33	0.06	2	.94
Extensor hallucis longus	2.66	2	.10	3.07	2	.07	0.17	2	.84	0.80	2	.47
Gastrocnemius medial head	**4.71**	**2**	**.02**	0.99	2	.39	1.83	2	.19	0.10	2	.90
Gastrocnemius lateral head	**6.88**	**2**	**.01**	0.99	2	.39	**6.10**	**2**	**.01**	2.53	2	.11
Soleus	**5.68**	**2**	**.01**	2.65	2	.10	2.48	2	.11	1.41	2	.27
Plantaris	0.91	2	.42	3.30	2	.06	0.64	2	.54	**5.88**	**2**	**.01**
Flexor hallucis longus	1.78	2	.20	0.61	2	.56	0.44	2	.65	0.74	2	.49
Tibialis caudalis	0.54	2	.59	1.11	2	.35	0.23	2	.80	1.19	2	.33
Peroneus longus	2.22	2	.14	0.97	2	.40	0.79	2	.47	0.82	2	.46
Peroneus brevis	0.02	2	.98	2.79	2	.10	0.31	2	.74	3.21	2	.07

Bold text indicates significant results $p < 0.05$

3.2.1 Fascicle length

The L_f of m. pectineus and m. tibialis cranialis were significantly different in all three species (Tables 3-8). Additionally, *B. suillus* had significantly longer fascicles in m. gluteus medius compared to both *G. capensis* and *C. h. natalensis.* The fascicles of m. piriformis were significantly shorter in *G. capensis* compared to *C. h. natalensis*. The L_f of m. gracilis anticus was significantly longer in *G. capensis* compared to that of *C. h. natalensis*. Additionally, trends in the L_f of m. extensor hallucis longus were observed between *G. capensis* and *B. suillus* (LSD: p=.03) as well as *G. capensis* and *C. h. natalensis* (LSD: p=.03). *Bathyergus suillus* had longer fascicles than *G. capensis*, while *G. capensis* had longer fascicles than *C. h. natalensis*. Furthermore, trends were observed in the L_f of m. plantaris between the two drumming species (LSD: p=.04) as well as between *B. suillus* and *C. h. natalensis* (LSD: p=.04) where *B. suillus* had the longest fascicles of the three species.

3.2.2 Muscle mass

Significant differences between *G. capensis* and *C. h. natalensis* were found in the M_M of mm. gluteus superficialis, semitendinosus and gluteofemoralis where *G. capensis* had the larger values. The M_M of the cranial head of m. biceps femoris and m. semimembranosus were significantly different in all three species, where *B. suillus* had the largest and *C. h. natalensis* had the smallest values in both muscles. The M_M of m. gracilis anticus as well as both the medial and lateral heads of m. gastrocnemius were significantly larger in both drumming species compared to *C. h. natalensis*. The M_M of m. soleus in *G. capensis* was the smallest of all three species and statistically smaller than that of *B. suillus*. Furthermore, trends were observed in the M_M of mm. gluteus medius (LSD: p=.02) and vastus lateralis (LSD: p=.04) between *G. capensis* and *C. h. natalensis* (Table 10) where *G. capensis* had larger values compared to *C. h. natalensis*. A significant difference between the sexes in *G. capensis* was observed where females had a larger m. gluteus medius M_M. The males of *C. h. natalensis* had a significantly smaller M_M in m. adductor longus compared to the females (Supplementary information).

3.2.3. Physiological cross-sectional area

The PCSA values of mm. piriformis, semitendinosus, gluteofemoralis, gracilis anticus and the lateral head of m. gastrocnemius were significantly larger in *G. capensis* compared to *C. h. natalensis*. Additionally, trends were observed in the PCSA values of the cranial head of m. biceps femoris and m. semimembranosus between *G. capensis* and *C. h. natalensis* where *G. capensis* had the larger value compared to *C. h. natalensis* for both muscles (LSD: p=.02 and LSD: p=.04, respectively). Furthermore, a sex difference was observed in *G. capensis* where females had a larger PCSA than males in m. semitendinosus (Supplementary information).

3.2.4. Architectural index (AI)

The L_f/L_M ratio of m. gluteus medius was significantly larger in *B. suillus* compared to both *G. capensis* and *C. h. natalensis*. Furthermore, the L_f/L_M ratios of m. piriformis and m. vastus intermedius, were significantly larger in *C. h. natalensis* compared to *G. capensis* (Fig. 4). Additionally, a sex difference was observed in the AI of *B. suillus* in m. vastus lateralis where females had the larger value. The males of *C. h. natalensis* had a larger L_f/L_M value in m. iliacus compared to the females. However, the females had the larger AI value in m. semitendinosus. The males of *G. capensis* had a larger AI in the lateral head of m. gastrocnemius while females had a larger value for m. plantaris (Supplementary information).
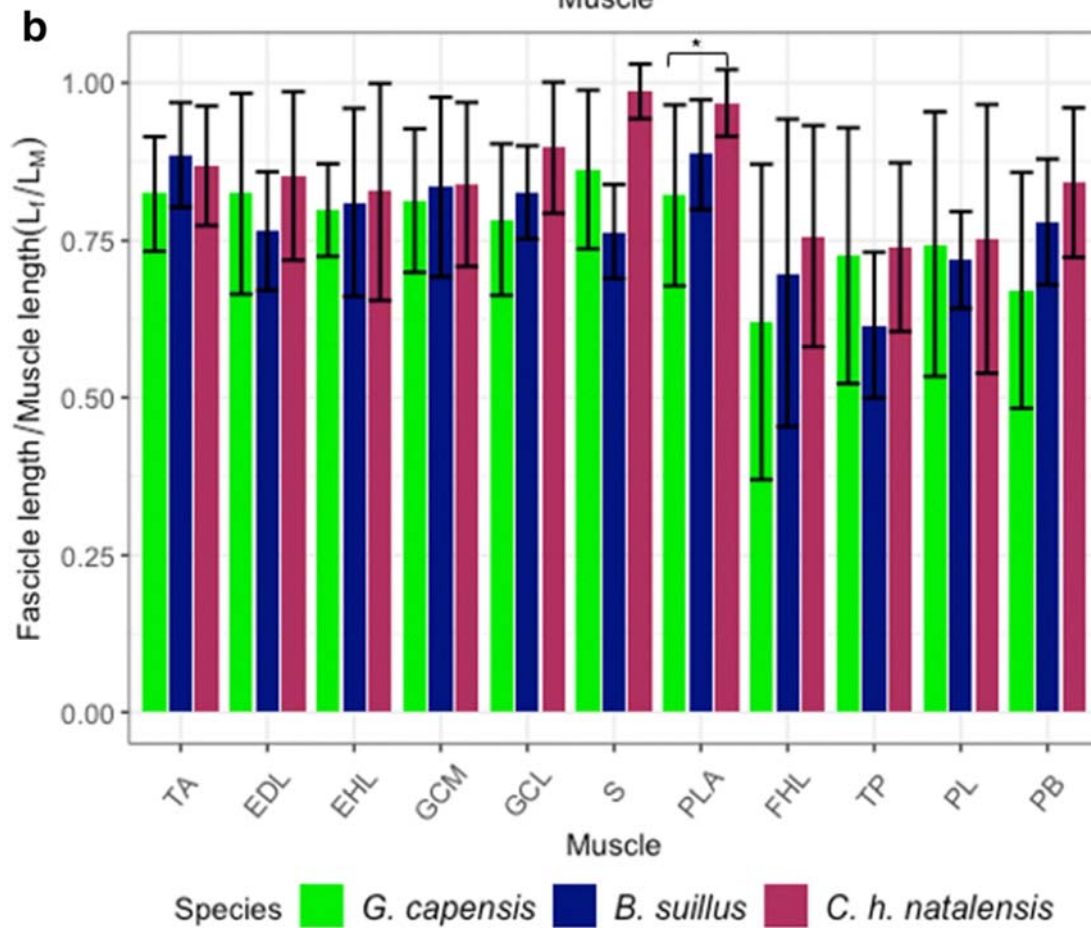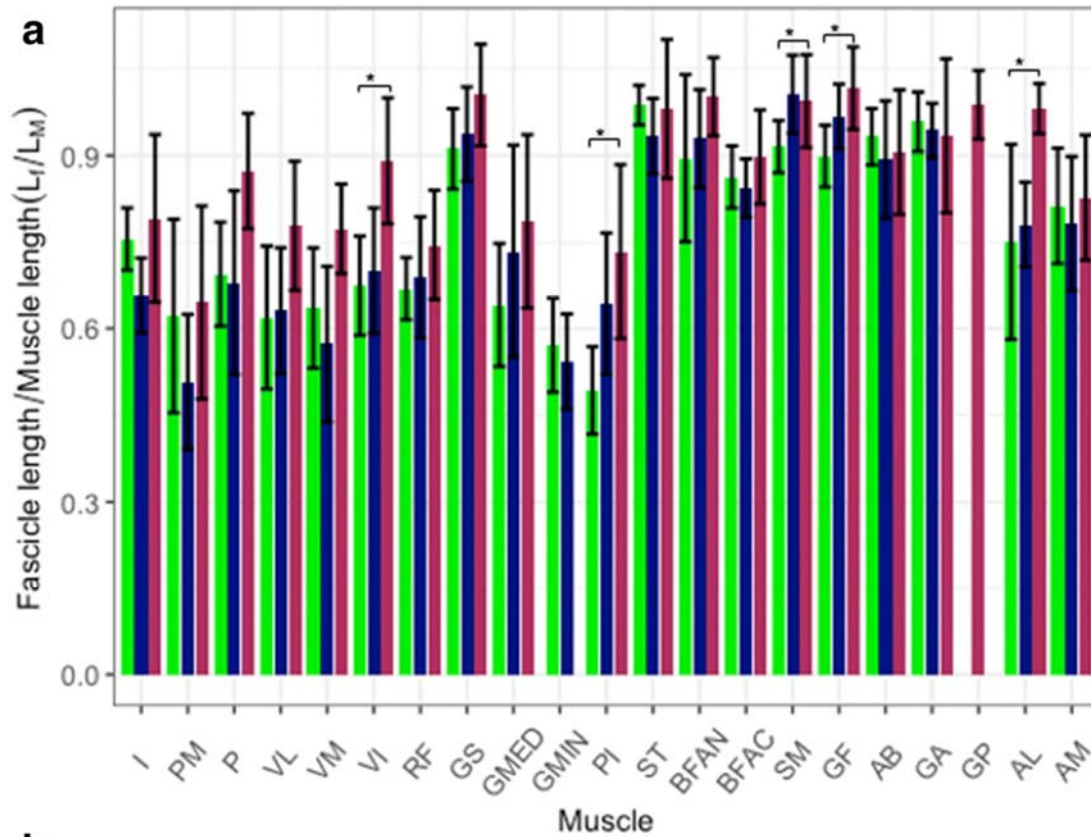
Figure 4. The mean (± standard deviation) architectural index of muscle fascicle length/muscle belly length (L_f/L_M) for the individual proximal (**A**) and distal (**B**) muscles of *G. capensis*, *B. suillus,* and *C. h. natalensis*. Higher values indicate a high capability for muscle shortening and a greater range of contraction.* indicates a significant difference of $p < .05$ between species Muscle abbreviations (as detailed in Tables 2-8): iliacus (I), psoas major (PM), pectineus (P), vastus lateralis (VL), vastus medialis (VM), vastus intermedius (VI), rectus femoris (RF), gluteus superficialis (GS), gluteus medius (GMED), gluteus profundus (GMIN), piriformis (PI), semitendinosus (ST), biceps femoris cranial head (BFAN), biceps femoris caudal head (BFAC), semimembranosus (SM), gluteofemoralis (GF), adductor brevis (AB), gracilis anticus (GA), gracilis posticus (GP), adductor longus (AL), adductor magnus (AM), tibialis cranialis (TA), extensor digitorium longus (EDL), extensor hallucis longus (EHL), gastrocnemius medial head (GCM), gastrocnemius lateral head (GCL), soleus (S), plantaris (PLA), flexor hallucis longus (FHL), tibialis caudalis (TP), peroneus longus (PL), and peroneus brevis (PB).

3.2.5. Functional space plot

The mean PCSA (normalized to mass, $PCSA/M_b^{0.67}$) of each muscle is plotted against the mean L_f (normalized to mass, $L_f/M_b^{0.33}$) per species in Figure 5. The bi-articular muscles of the hip extensor and knee flexor groups (Mm. semitendinosus, semimembranosus, cranial heads of m. biceps femoris) as well as the hip adductors (Mm. gracilis anticus and adductor brevis) and the hip extensor (m. gluteofemoralis*)* of both drumming species are in the high shortening capacity (lower right) quadrant of Figure 5. In contrast, m. gracilis anticus of *C. h. natalensis* was in the generalized (lower left) quadrant. Additionally, the mm. gracilis anticus and adductor brevis of *G. capensis* were the farthest to the right in comparison to the other two species. However, m. semimembranosus and the cranial head of m. biceps femoris of *B. suillus* were the furthest to the right compared to the other two species, indicating that these muscles may have a high shortening capacity.
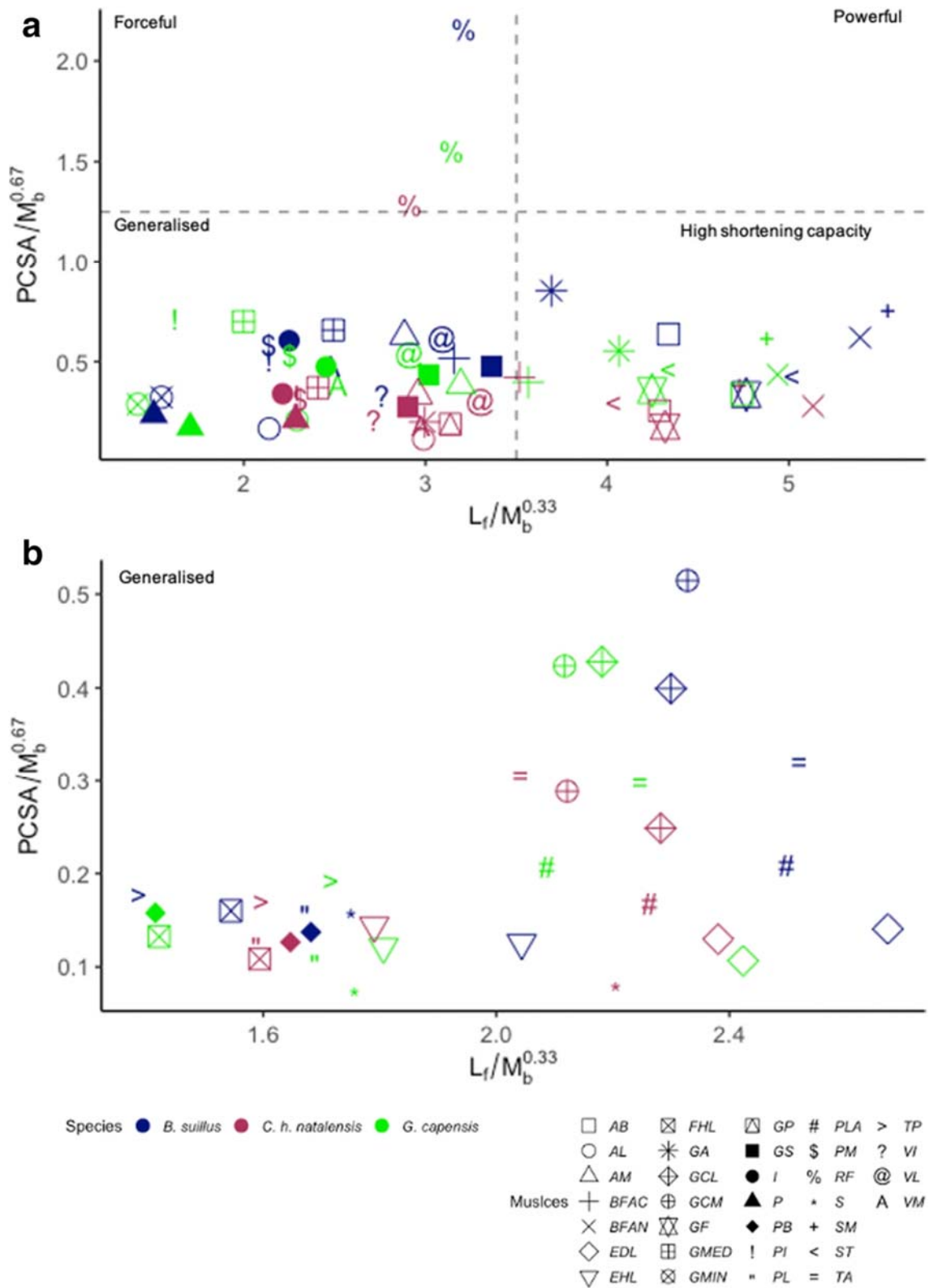
Figure 5. Physiological cross-sectional area, normalized to body mass (PCSA/BM$^{0.67}$) as a function of resting fascicle length normalized to body mass (LF/BM$^{0.33}$) of the individual proximal (**A**) and distal (**B**) muscles for G.

capensis, *B. suillus*, and *C. h. natalensis*. The horizontal dashed line separates muscles with high (above) versus low (below) force capability, while the vertical dashed line separates muscles with high (right) versus low (left) shortening capability. Muscles with both high force and high shortening capabilities are capable of high-power outputs (right upper quadrant). For panel B all these distal muscles are in the lower left quadrant of panel A but are shown separately for ease of reference. Muscle abbreviations (as detailed in Tables 3-8) iliacus (I), psoas major (PM), pectineus (P), vastus lateralis (VL), vastus medialis (VM), vastus intermedius (VI), rectus femoris (RF), gluteus superficialis (GS), gluteus medius (GMED), gluteus profundus (GMIN), piriformis (PI), semitendinosus (ST), biceps femoris cranial head (BFAN), biceps femoris caudal head (BFAC), semimembranosus (SM), gluteofemoralis (GF), adductor brevis (AB), gracilis anticus (GA), gracilis posticus (GP), adductor longus (AL), adductor magnus (AM), tibialis cranialis (TA), extensor digitorium longus (EDL), extensor hallucis longus (EHL), gastrocnemius medial head (GCM), gastrocnemius lateral head (GCL), soleus (S), plantaris (PLA), flexor hallucis longus (FHL), tibialis caudalis (TP), peroneus longus (PL), and peroneus brevis (PB).

4.   DISCUSSION

Muscle architecture provides insight into the functional capability of individual muscles as well as synergistic muscle groups. This includes the relationships between physical properties and force as well as velocity of contraction (Lieber and Ward 2011). The study of homologous muscles in closely related species can further provide insight into functional specialisation due to different functional demands (Rosin and Nyakatura 2017).

The PCSA values typically increase with an increasing body mass (Kikuchi 2010), which was observed in all three species studied here. Therefore, when comparing the species, body mass was used as a covariate to take in to account the large difference in body mass observed between the three species studied here. Although *B. suillus* had the largest values of all the parameters per muscle group and individual muscles, with a few exceptions, significant differences were most often observed between the rapidly drumming *G. capensis* and the non-drumming *C. h. natalensis.* This may therefore be

indicative of an adaptation for the high rate of hind foot drumming seen in *G. capensis* (Narins et al. 1992).

Typically, the longer the fascicle, the smaller the PCSA value, thereby indicating an adaptation for increased velocity of contraction. In contrast, higher PCSA values are indicative of more forceful muscle contraction (Lieber 2000; Wilson and Lichtwark 2011). If both properties are present, the muscle is regarded as powerful, thereby exhibiting both fast and forceful contraction (Zajac 1989,1992; Lieber 2011). The PCSA values of the hip extensors, hip adductors, knee extensors, and knee flexors of *G. capensis* were significantly larger than that of *C. h. natalensis.* Additionally, the knee flexors and hip extensors of the two drumming species were present in the upper right quadrant of Figure 3, indicating that they are capable of a high power output. This may be indicative of adaptations for hind foot drumming as hip extension and knee flexion are key actions in hind foot drumming (Randall 2014). Furthermore, the hip adductors of *G. capensis* extended further into the lower right quadrant of Figure 3, indicating that they are likely to be adapted for increased shortening capacity while simultaneously having large range of motion (Rupert et al. 2015). This feature may facilitate the rapid rate of drumming observed in *G. capensis*.

The m. gracilis anticus was the only muscle to have significantly larger values in *G. capensis* compared to *C. h. natalensis* in all three muscle architecture parameters (L_f, M_M, PCSA) analyzed. Additionally, while not statistically significant between the species, *G. capensis* had the highest value for the L_f/L_M ratio in m. gracilis anticus (0.96) of the three species. Furthermore, it features in the high shortening capacity quadrant of the functional space plot of the two drumming species but not in the non-drumming *C. h. natalensis* (Fig. 5). Musculus gracilis anticus acts as both a knee flexor and hip adductor and was the only muscle to show a macroscopic difference between the species studied here. Sahd et al. (2019) observed two parts namely m. gracilis anticus and m. gracilis posticus in the non-drummer but a single

muscle in both the drumming species. Therefore, m. gracilis anticus is potentially a key muscle involved in the facilitation of hind foot drumming.

High values of the L_f/L_M ratio (greater than 0.5) indicate the ability of a muscle to move a joint through a large range of motion and with a greater range of contraction (Olson et al. 2018; Rupert et al. 2015). The L_f as well as the ratio of L_f/L_M of m. piriformis in *G. capensis* were significantly smaller than that of non-drumming *C. h. natalensis.* Small values in both these properties indicate the potential for low contraction velocity which implies that the m. piriformis of *G. capensis* acts as a stabilizer for the hip joint during drumming. Additionally, m. piriformis seems to be adapted for force production rather than increased contraction of velocity as the PCSA was significantly larger in *G. capensis* compared to *C. h. natalensis*. The L_f/L_M ratio of m. semimembranosus was significantly higher in both *B. suillus* and *C. h. natalensis* compared to *G. capensis* indicating that *G. capensis* may be using other hip extensors (such as the cranial head of m. biceps femoris) for rapid contraction. Interestingly, in the two drumming species, the muscles with the highest L_f/L_M ratio were two bi-articular muscles namely m. semitendinosus (0.99) in *G. capensis* and m. semimembranosus (1.01) in *B. suillus* (both hip extensors and knee flexors). while in *C. h. natalensis,* the highest L_f/L_M ratio was observed in m. gluteofemoralis (1.02; hip extensor). This difference in the functionality of the muscles with the highest contraction ability and range of motion between the drumming and non-drumming species may be due to the repetitive flexion of the knee during hind foot drumming.

Several muscles showed differences in various muscle architecture parameters between sexes in the present study. The sex differences observed in *G. capensis* could likely be due to the difference in drumming rate observed between the males and females (26 beats/second in males and 15 beats/second in females; Van Sandwyk and Bennett 2005) as no physical sexual dimorphism is reported in this species (Bennett and Faulkes 2000). The sex differences observed in *B. suillus* and *C. h. natalensis* may be due to a difference in body mass where males are larger than females (Jarvis and Bennett 1991).

The proximal to distal gradient of muscle mass distribution seen in all three species studied here is a consistent feature in cursorial animals such as the ostrich (*Struthio camelus;* Smith et al. 2006) horse (*Equus caballus;* Payne et al. 2005), cheetah (*Acinonyx jubatus*), and greyhound (*Canis lupis familiaris*; Hudson et al. 2011). The proximal to distal reduction of muscle mass can reduce the amount of muscular work required to accelerate and decelerate the limb (Lee et al. 2004; Hudson et al. 2011). The hip extensors and knee flexors comprised approximately 40% each of the total hind limb muscle mass in all three species studied here. This feature is similar to the cheetah where the hip extensors and knee flexors comprised approximately 43% and 30%, respectively of the total limb muscle mass (Hudson et al. 2011). This may indicate that the proximal hind limb muscles are adapted to produce measurable mechanical advantage.

Limitations to this study include the fact that the exact age and health status of the samples were unknown as all animals were wild caught. Furthermore, as two-thirds of the samples were already fixed prior to receipt, the authors could not change hip and knee joint angle positions but consistently chose the limb (left or right) with the knee joint angle closest to 90°. The present study also did not examine muscular moment arms, muscle fiber types, or tendon characteristics, which can be included in future studies to further help demonstrate muscular adaptations for hind foot drumming.

5.   CONCLUSION

Adaptations to the hind limb muscle architecture of African mole-rats for hind foot drumming are unknown. Therefore, the internal structure of 32 hind limb muscles was evaluated in two drumming and one non-drumming species of Bathyergidae. With body mass accounted for in the statistical analysis, most significant differences for the various muscle architecture parameters analyzed in synergistic muscle groups and individual muscles were observed between the rapid drumming *G. capensis* and the non-drumming *C. h. natalensis*. The hip extensors and knee flexors of both the drumming species were shown to be capable of higher power output compared to the non-drumming

species. M. gracilis anticus may play a key role in facilitating hind foot drumming as it was the only muscle to be significantly different in *G. capensis* and *C. h. natalensis* in all three muscle architecture parameters analyzed. Additionally, it features in the high shortening capacity quadrant of the functional space plot of the two drumming species but not the non-drumming *C. h. natalensis*.

ACKNOWLEDGEMENTS

DECLARATIONS:

Ethical clearance:

Ethical approval to use the specimens was obtained from the Stellenbosch University Research Ethics Committee: Animal Care and Use (REC: ACU; SU-ACUM 16-00005)

Data availability statement:

The data that support the findings of this study are available from the corresponding author upon reasonable request.

Funding information:

Author contributions

Lauren Sahd performed the analysis and drafted the manuscript. Nigel Bennett provided the samples and edited the manuscript. Sanet Kotzé was the principle investigator, designed the project and edited the manuscript.

Conflict of interest:

The authors have no conflict of interest to declare.

REFERENCES

Allen V, Elsey RM, Jones N, Wright J, Hutchinson JR (2010) Functional specialization and ontogenetic scaling of limb anatomy in *Alligator mississippiensis*. J Anat 216:423-445

Bennett NC, Faulkes CG (2000) African Mole-rats: Ecology and Eusociality. Cambridge University Press, Cambridge

Bennett NC, Jarvis JUM (1988) The reproductive biology of the Cape mole-rat, *Georychus capensis* (Rodentia: Bathyergidae). J Zool 214: 95-106

Bennett NC, Maree S, Faulkes CG (2006) *Georychus capensis.* Mammal Species 799: 1-4

Brown M, Louw DG (2007) Automatic panoramic image stitching using invariant features. Int J Comput Vis: 74:59-73

Burkholder TJ, Fingad, B, Baron S, Lieber R (1994) Relationship between muscle fiber types and sizes and muscle architectural properties in the mouse hindlimb. J Morphol 221: 177-190

Charles JP, Cappellari O, Spence AJ, Hutchinson JR, Wells DJ (2016) Musculoskeletal geometry, muscle architecture and functional specialisations of the mouse hindlimb. PLoS ONE 11:e0147669

Eng CM, Smallwood LH, Rainiero MP, Lahey M, Ward SR, Lieber RL (2008) Scaling of muscle architecture and fiber types in the rat hindlimb. J Exp Biol 211: 2336-2345

Francescoli G (2000) Sensory capabilities and communication in subterranean rodents. In: Lacey EA, Patton JL, Cameron GN (eds) Life Underground: The Biology of Subterranean Rodents. University of Chicago Press, Chicago, pp 111-144

Fukunaga T, Roy RR, Shellock FG, Hodgson JA, Edgerton VR (1996) Specific tension of human plantar flexors and dorsiflexors. J Appl Physiol (1996) 80: 158-65

Hart L, O'Riain MJ, Jarvis JUM, Bennett NC (2006) The pituitary potential for opportunistic breeding in the Cape dune mole-rat, *Bathyergus suillus.* Physiol Behav 88: 615-619

Hill PSM (2009) How do animals use substrate-borne vibrations as an information source? Naturwissenschaften 96: 1355-1371

Hudson PE, Corr SA, Payne-Davis RC, Clancy SN, Lane E, Wilson AM (2011) Functional anatomy of the cheetah (*Acinonyx jubatus*) hindlimb. J Anat 218: 363-374

Jarvis JUM, Bennett NC (1991) Ecology and behaviour of the family Bathyergidae. In: Sherman PW, Jarvis JUM, Alexander RD (eds) The Biology of the Naked Mole-rat. Princeton University Press, New York, pp 66-96

Kikuchi Y (2010) Comparative analysis of muscle architecture in primate arm and forearm. Anat Histol Embryol 39: 93-106

Kikuchi Y, Kuraoka A (2014) Differences in muscle dimensional parameters between non-formalin-fixed (freeze-thawed) and formalin-fixed specimen in gorilla (*Gorilla gorilla*). Mammal Study 39: 65-72

Lacey EA, Patton JL, Cameron GN (eds) (2000) Life Underground: The Biology of Subterranean Rodents. University of Chicago Press, Chicago

Lee DV, Startebake EF, Walter RM, Carrier DR (2004) Effects of mass distribution on the mechanics of level trotting in dogs. J Exp Biol 207: 1715-1728

Lieber RL (1993) Skeletal muscle architecture: implications for muscle function and surgical tendon transfer. J Hand Ther 4: 105-113

Lieber RL, Friden J, (2000) Functional and clinical significance of skeletal muscle architecture. Muscle & Nerve 23: 1647-1666

Lieber RL, Ward SR (2011) Skeletal muscle design to meet functional demands. Philos Trans R Soc B 366: 1466-1476

Maganaris CN, Baltzopoulos V, Ball D, Sargeant AJ (2001) *In vivo* specific tension of human skeletal muscle. J Appl Physiol 90:865-72

Martin ML, Warburton NM, Travouillon KJ, Flemming PA (2019) Mechanical similarity across ontogeny of digging muscles in an Australian marsupial (*Isoodon fusciventer*). J Morphol 280: 423-435

Mason MJ, Narins PM (2001) Seismic signal use by fossorial mammals. Am J Zool 41: 1171-1184

Mason MJ, Narins PM (2010) Seismic sensitivity and communication in subterranean mammals In: O'Connell-Rodwell CE (ed) The Use of Vibrations in Communication: Properties, Mechanisms and Function across Taxa. Transworld Research Network, Kerala, pp 121-139

Medler S (2002) Comparative trends in shortening velocity and force production in skeletal muscle. Am J Physiol Regul Integr Comp 283: R368-R378

Mendez J, Keyes A (1960) Density and composition of mammalian muscle. Metabolism 9: 184-188

Moore AL, Budny JE, Russell, AP, Butcher MT (2013) Architectural specialisation of the intrinsic thoracic limb musculature of the American badger (*Taxidea taxus*). J Morphol 274: 35-48

Myatt JP, Crompton RH, Trope SKS (2011) Hindlimb muscle architecture in non-human great apes and a comparison of methods for analysing inter-species variation. J Anat 219: 150-166

Narins PM, Reichman OJ, Jarvis JUM, Lewis ER (1992) Seismic signal transmission between burrows of the Cape mole-rat, *Georychus capensis.* J Comp Physiol A 170: 13-21

Olsen RA, Glenn ZD, Cliffe RN, Butcher MT (2018) Architectural properties of sloth forelimb muscles (Pilosa: Bradypodia). J Mammal Evol 25: 573-585

Payne RC, Hutchinson JR, Robilliard JJ, Smith NC, Wilson AM (2005) Functional specialisation of pelvic limb anatomy in horses (*Equus caballus*). J Anat 206: 557-574

R Core Team (2013) R: A language and environment for statistical computing. R Foundation for Statistical Computing, Vienna. URL http://www.R-project.org/

Randall JA (2001) Evolution and function of drumming as communication in mammals. Am Zool 41: 1143-1156

Randall JA (2010) Drummers and stompers: vibrational communication in mammals. In: O'Connell-Rodwell CE (ed) The Use of Vibrations in Communication: Properties, Mechanisms and Function across Taxa. Transworld Research Network, Kerala, pp100-120.

Randall JA (2014) Vibrational communication: spiders to kangaroo rats. In: Witzany G (ed) Biocommunication of Animals. Springer, Dordrecht, pp103-133

Rose JA, Sandefur M, Huskey S, Demler JL, Butcher MT (2013) Muscle architecture and out-force potential of the thoracic limb in the Eastern mole (*Scalopus aquaticus*). J Morphol 274:1277-1287

Rosin S, Nyakatura JA (2017) Hind limb extensor muscle architecture reflects locomotor specialisations of a jumping and a striding quadrupedal caviomorph rodent. Zoomorphology 136: 267-277

Rupert JE, Rose JA, Organ JM, Butcher MT (2015) Forelimb muscle architecture and myosin isoform composition in the groundhog (*Marmota monax*). J Exp Biol 218: 194-205

Sacks RD, Roy RR (1982) Architecture of the hind limb muscle of cats: Functional significance. J Morphol 173: 194-195

Sahd L, Bennett NC, Kotzé SH (2019) Hind foot drumming: morphological adaptations of the muscles and bones of the hind limb in three African mole-rat species. J Anat 235: 811-824

Schneider CA, Rasband WS, Eliceiri KW (2012) NIH Image to ImageJ: 25 years of image analysis Nat methods 9: 671-675

Smith NC, Wilson AM, Jespers KJ, Payne RC (2006) Muscle architecture and functional anatomy of the pelvic limb of the ostrich (*Struthio camelus*). J Anat 209:765-779

Wickham H (2016) ggplot2: Elegant Graphics for Data Analysis. Springer-Verlag, New York

Wickiewicz TL, Roy RR, Powell PL, Edgerton VR (1983) Muscle architecture of the human lower limb. Clin Orthop Rel Res 179:275–283

Williams SB, Payne RC, Wilson AM (2007) Functional specialization of the pelvic limb of the hare (*Lepus europeus*). J Anat 210: 472-490

Wilson A, Lichtwark G (2011) The anatomical arrangement of muscle and tendon enhances limb versatility and locomotor performance. Philos Trans R Soc B 366: 1540-1553

Zajac FE (1989) Muscle and tendon: properties, models, scaling and application to biomechanics and motor control. Crit Rev Biomed Engng 17:359-411

Zajac FE (1992) How musculotendon architecture and joint geometry affect the capacity of muscles to move and exert force on objects: a review with application t arm and forearm tendon transfer design. J Hand Surg Am 17: 799-804